doi:10.1093/brain/awab009 BRAIN 2021: Page 1 of 14 | 1

BRAIN
A JOURNAL OF NEUROLOGY

Cognitive impairment and altered cerebral glucose metabolism in the subacute stage of COVID-19

Jonas A. Hosp,[1,†] Andrea Dressing,[1,2,†] Ganna Blazhenets,[3] Tobias Bormann,[1] Alexander Rau,[4] Marius Schwabenland,[5] Johannes Thurow,[3] Dirk Wagner,[6] Cornelius Waller,[7] Wolf D. Niesen,[1] Lars Frings,[3] Horst Urbach,[4] Marco Prinz,[5,8,9] Cornelius Weiller,[1,2] Nils Schroeter[1,†] and Philipp T. Meyer[3,†]

[†]These authors contributed equally to this work.

During the severe acute respiratory syndrome coronavirus 2 (SARS-CoV-2) pandemic, neurological symptoms increasingly moved into the focus of interest. In this prospective cohort study, we assessed neurological and cognitive symptoms in hospitalized coronavirus disease-19 (COVID-19) patients and aimed to determine their neuronal correlates. Patients with reverse transcription-PCR-confirmed COVID-19 infection who required inpatient treatment primarily because of non-neurological complications were screened between 20 April 2020 and 12 May 2020. Patients (age $>$ 18 years) were included in our cohort when presenting with at least one new neurological symptom (defined as impaired gustation and/or olfaction, performance $<$ 26 points on a Montreal Cognitive Assessment and/or pathological findings on clinical neurological examination). Patients with $\geqslant$2 new symptoms were eligible for further diagnostics using comprehensive neuropsychological tests, cerebral MRI and ^{18}fluorodeoxyglucose (FDG) PET as soon as infectivity was no longer present. Exclusion criteria were: premorbid diagnosis of cognitive impairment, neurodegenerative diseases or intensive care unit treatment. Of 41 COVID-19 inpatients screened, 29 patients (65.2 ± 14.4 years; 38% female) in the subacute stage of disease were included in the register. Most frequently, gustation and olfaction were disturbed in 29/29 and 25/29 patients, respectively. Montreal Cognitive Assessment performance was impaired in 18/26 patients (mean score 21.8/30) with emphasis on frontoparietal cognitive functions. This was confirmed by detailed neuropsychological testing in 15 patients. ^{18}FDG PET revealed pathological results in 10/15 patients with predominant frontoparietal hypometabolism. This pattern was confirmed by comparison with a control sample using voxel-wise principal components analysis, which showed a high correlation (R^2 = 0.62) with the Montreal Cognitive Assessment performance. Post-mortem examination of one patient revealed white matter microglia activation but no signs of neuroinflammation. Neocortical dysfunction accompanied by cognitive decline was detected in a relevant fraction of patients with subacute COVID-19 initially requiring inpatient treatment. This is of major rehabilitative and socioeconomic relevance.

1 Department of Neurology and Clinical Neuroscience, Medical Center, University of Freiburg, Faculty of Medicine, University of Freiburg, Freiburg, Germany
2 Freiburg Brain Imaging Center, Medical Center, University of Freiburg, Faculty of Medicine, University of Freiburg, Freiburg, Germany
3 Department of Nuclear Medicine, Medical Center, University of Freiburg, Faculty of Medicine, University of Freiburg, Freiburg, Germany
4 Department of Neuroradiology, Medical Center, University of Freiburg, Faculty of Medicine, University of Freiburg, Freiburg, Germany
5 Institute of Neuropathology, Faculty of Medicine, University of Freiburg, Freiburg, Germany

Received July 13, 2020. Revised September 25, 2020. Accepted October 29, 2020.

6 Division of Infectious Diseases, Department of Internal Medicine II, Medical Center, University of Freiburg, Faculty of Medicine, University of Freiburg, Freiburg, Germany
7 Department of Internal Medicine I, Medical Center, University of Freiburg, Faculty of Medicine, University of Freiburg, Freiburg, Germany
8 Center for Basics in NeuroModulation (NeuroModulBasics), Faculty of Medicine, University of Freiburg, Freiburg, Germany
9 Signalling Research Centres BIOSS and CIBSS, University of Freiburg, Freiburg, Germany

Correspondence to: Jonas A. Hosp, MD
University Medical Center Freiburg
Department of Neurology and Neuroscience
Breisacher Str. 64, 79106 Freiburg, Germany
E-mail: jonas.hosp@uniklinik-freiburg.de

Keywords: COVID-19; cognition; neurology; 18FDG PET; Montreal Cognitive Assessment

Abbreviations: ADNI = Alzheimer's disease neuroimaging initiative; COVID-19 = coronavirus disease-19; ^{18}FDG = ^{18}fluorodeoxyglucose; ICU = intensive care unit; MoCA = Montreal Cognitive Assessment; PCA = principal components analysis; SARS-CoV-2 = severe acute respiratory syndrome coronavirus 2; SPM = statistical parametric mapping; SUV = standardized uptake value

Introduction

During the severe acute respiratory syndrome coronavirus 2 (SARS-CoV-2) pandemic, the emergence of neurological symptoms increasingly moved into the focus of interest.[1,2] Altogether, 37% (inpatients[3]) to 84% [intensive care unit (ICU) treatment[4]] of coronavirus disease-19 (COVID-19) patients show neurological symptoms, and these symptoms are not restricted to a severe course of disease. In line with these observations, elevated serum markers of axonal injury (neurofilament light chain protein) and astrocytic activation (glial fibrillary acidic protein, GFAP) have been detected in mild-to-moderate[5] and moderate-to-severe cases of COVID-19,[6] indicating an effect on the CNS. Apart from embolic cerebral infarctions and the involvement of peripheral nerves, 20–70% of patients with COVID-19 show a quantitative or qualitative disturbance of consciousness during the acute phase.[3,4] Peri-infectious encephalopathies can lead to cognitive impairment or pass into dementia[7,8] and have been observed in past coronavirus-related epidemics.[9] The neuroinvasive propensity of human betacoronavirus clades has been described repeatedly.[10-12] Olfactory and gustatory dysfunction, which occurs in up to 85%[13,14] of COVID-19 patients, could indicate trafficking of the virus into the CNS[12] as demonstrated in murine models of coronavirus infection.[11] Furthermore, a systemic inflammatory response to SARS-CoV-2 infection may elicit a 'cytokine-storm'[15] that could alter homeostatic processes within the CNS similar to septic encephalopathy.[7]

Guided by these considerations and with the intention to assess the impact of SARS-CoV-2 infection on the CNS, COVID-19 inpatients at the subacute stage were examined for disturbances of gust, olfaction and other neurological signs. The cognitive state was tested using the Montreal Cognitive Assessment (MoCA). Patients showing more than one new neurological symptom ($\geqslant 2$) were eligible for further investigations: a neuropsychological test battery, analysis of the CSF, structural MRI and PET with ^{18}fluorodeoxyglucose (^{18}FDG) to assess regional cerebral glucose metabolism. ^{18}FDG PET is not only an established biomarker of neuronal function[16] and neuronal injury,[17] respectively, but also of CNS inflammation even in the absence of typical MRI findings.[18] Using this multimodal approach, we aimed to comprehensively characterize the neurological sequelae of COVID-19 in the subsample of patients affected severely enough to require inpatient treatment.

Materials and methods

Study design and participants

In this study, we investigated the neurological and neuro-cognitive sequelae of COVID-19. We report data from a monocentric neuro-COVID-19 register, which includes prospectively examined patients with reverse transcription (RT)-PCR-confirmed SARS-CoV2 infection and new neurological symptoms, consecutively admitted for inpatient treatment to the Department of Internal Medicine of University Hospital Freiburg between 20 April 2020 and 12 May 2020. All available patients were screened. Patients were examined by a board-certified (J.H.) or experienced (>5 years training, N.S. and A.D.) neurologist as part of the clinical routine. Examination included medical history, comprehensive neurological examination, tests for olfaction and gustation disturbance and a test for cognitive deficits (MoCA). Reasons for inpatient treatment were identified.

Inclusion criteria were: a positive SARS-CoV2 RT-PCR result from nasopharyngeal swabs, age >18 years and presentation of at least one newly acquired neurological symptom. The following neurological symptoms were assessed systematically: (i) anamnestic or measured disturbance of olfaction or gustation; (ii) cognitive impairment reflected by a MoCA score < 26; and (iii) affections of other cranial nerves or the CNS on clinical neurological examination. Patients included in the register and

presenting signs of a possible COVID-19-related encephalopathy (defined by two or more new neurological symptoms) were eligible for extended structural and functional imaging (cerebral MRI and ^{18}FDG PET) and a neuropsychological test battery as soon as infectivity was no longer present according to the in-house guidelines of the University Hospital Freiburg (two negative SARS-CoV2 RT-PCRs in sequence or 14 days after the last positive RT-PCR and 2 days without any COVID-19-related symptoms). Exclusion criteria were a previous diagnosis of any neurodegenerative or neuroimmunological disorder or exclusive treatment in the ICU, to avoid confounding cognitive performance due to the ICU environment. Past ICU treatment was not an exclusion criterion if the patients were treated on a normal ward at the time of screening/inclusion. The register study was approved by the local ethics committee (EK 211/20). Written, informed consent for this study was obtained from all participants in accordance with the Declaration of Helsinki.

Outcomes

Olfaction and gustation

Olfaction was assessed using Burghart Sniffin'-Sticks® (Burghart Messtechnik GmbH), an established screening test for olfactory performance.[19] Ammonium was used to assess trigeminal function (normosmia: 11–12 correct odours; hyposmia: 7–10 correct odours; anosmia: <6 correct odours). Gustatory perception was assessed by the targeted administration of standardized solutions (10% sucrose, 5% citric acid, 7.5% NaCl and 0.05% quinine) in accordance with current German guidelines.[20]

Cognitive functions

Cognitive functions were assessed using the German version of the MoCA (version 7.1, www.mocatest.org[21]) the cut-off score for cognitive impairment was defined as <26 as reported previously.[21] This cut-off value was established in a large cohort of patients with Alzheimer's dementia, mild cognitive impairment and healthy controls as the most sensitive (90%) for distinguishing between healthy controls and patients with mild cognitive impairment. Correction for years of education was performed for the global MoCA score ($+1$ point in the case of $\leqslant 12$ years of education). Cognitive deficits were further evaluated by domain scores based on single item scores.[21] MoCA domain scores were calculated as means of single item scores and comprised subscores for orientation (spatial and temporal orientation), attention (digit span, letter A tapping and subtraction), executive function (trail making, abstraction and word fluency), visuoconstructive function (cube copying and clock drawing) and language (naming, sentence repetition and memory: delayed word recall). Domain scores were not adjusted for years of education.

The extensive neuropsychological test battery covered the domains of memory, attention and executive functions (for a detailed description of the comprehensive cognitive battery see Supplementary material and Supplementary Table 1). The MoCA and neuropsychological test battery results are reported as mean (± standard deviation, SD). For neuropsychological testing, *z*-scores were established based on the means and standard deviations for each outcome variable and stratified by age and education where possible; impaired performance on a test was defined as –1.5 SD below the mean of the respective normative group.[22]

Cerebral MRI

Patients underwent MRI on a 3 T scanner (Magnetom Prisma, Siemens Medical Solutions) with a 64-channel head coil including the following sequences: sagittal 3D T_1-weighted magnetization prepared rapid gradient echo (MP-RAGE) before and after contrast agent administration, sagittal 3D FLAIR SPACE (sampling perfection with application-optimized contrasts using different flip angle evolutions), axial susceptibility-weighted imaging (SWI), axial proton density + T_2 double echo, dynamic susceptibility contrast (DSC) perfusion imaging and diffusion mesoscopic imaging (DMI) with 61 diffusion-encoding directions and b-factors of 1000 and 2000 s/mm^2, evaluated by a board-certified neuroradiologist (H.U.). A voxel-based and atlas-based DSC-perfusion analysis was performed with 30 age-matched subjects as a control group (Supplementary material) to assess potential changes in brain perfusion.

^{18}FDG PET imaging

All PET scans were acquired on a fully digital Vereos PET/CT scanner (Philips Healthcare). PET emission data were acquired 50 min after the injection of 215 (13) MBq ^{18}FDG for 10 min (Supplementary material). For single subject visual assessments, highly standardized displays of 30 transaxial ^{18}FDG PET slices (in native space) covering each patient's entire brain were created. All scans were uniformly displayed using a hot metal colour scale with the maximum being set to 1.8× mean uptake in brain parenchyma (minimum set to 0.09 normalized uptake, i.e. 5% of maximum for background suppression). Two experienced nuclear medicine physicians (rater 1: P.T.M., board-certified specialist in nuclear medicine and >20 years of experience in brain PET; rater 2: J.T., 4 years of experience) independently rated all individual scans on an ordinal three-step scale (0, normal; 1, mildly abnormal; 2, severely abnormal) and noted the dominant finding. A final, binary consensus was reached regarding normal/abnormal.

Visual assessments were conducted in analogy to current practice guidelines.[23] After the exclusion of possible artefacts (e.g. motion and attenuation correction), both raters systematically inspected the cortical, subcortical, brainstem and cerebellar structures for deviations (uptake level and symmetry) from the well-known physiological ^{18}FDG uptake pattern in adults. Both raters were trained in the PET system employed (using identical parameters) and are competent to consider physiological changes in their visual ratings. Most importantly, this included declines in cerebral ^{18}FDG uptake due to normal ageing (e.g. mild frontal decline in older patients) and atrophy. To this end, the raters were informed about the ages of the patients and had access to MRI scans to consider partial volume effects due to atrophy. The raters were also informed about cerebral (micro-) infarctions in four patients (see below) and instructed to rate abnormalities going beyond those structural defects and possibly expectable diaschisis.

The use of a fully digital PET/CT system provides superior image quality and spatial resolution.[24] However, given the recent advent of this technique, a normative database of healthy controls is not yet available. Thus, we selected age-matched control patients (n = 45) scanned under identical conditions from our database for statistical comparisons, in whom somatic CNS diseases were carefully excluded (Supplementary material).

Based on earlier studies demonstrating the superior value of disease-specific spatial covariance patterns for diagnosis, prognosis and monitoring of various diseases,[25] we used principal components analysis (PCA) to explore whether a spatial covariance pattern exists in COVID-19 and how this relates to cognitive function. This approach operates on the notion that localized disease processes ought to engage multiple, interacting brain regions that are widely distributed over the whole brain. Opposed to conventional regional or voxel-based statistical PET analyses, PCA offers the additional advantage that it does not require the explicit definition of a non-affected reference region for count rate normalization, which is currently unknown in COVID-19.

All processing steps were implemented with an in-house pipeline in MATLAB (MathWorks, Inc., Natick, Massachusetts, USA) and statistical parametric mapping (SPM12) software (www.fil.ion.ac.uk/spm). ^{18}FDG PET scans were spatially normalized to an in-house ^{18}FDG PET template in Montreal Neurological Institute space and smoothed with an isotropic Gaussian kernel of 10 mm full-width at half-maximum. Scaled subprofile model PCA was used to generate a scaled subprofile model pattern based on group discrimination between COVID-19 and control patients using the Scanvp/SSMPCA toolbox[25] as previously described[26] (Supplementary material). For correlation with visual reads and cognitive scores (MoCA adjusted for years of education), each individual's pattern expression score of the COVID-19-related spatial covariance pattern was evaluated by the topographic profile rating algorithm involving computation of the internal vector product of the subject's residual profile vector and the pattern vector.[27] Furthermore, for exploratory analyses of the physiological basis of the observed covariance patterns (i.e. in terms of absolute regional glucose metabolism), we assessed the mean ^{18}FDG uptake (expressed lean body weight- and plasma glucose-adjusted standardized uptake value, SUV; Supplementary material) in the voxel with 10% highest weights, both for negative (relative hypometabolism) and positive (relative hypermetabolism) voxel weights.

Finally, for validation purposes, we conducted two confirmatory analyses: Individual scans underwent the same preprocessing as described for the PCA analysis. First, we performed a conventional group analysis using SPM. A two-sampled *t*-test between the COVID-19 group and control group was calculated after proportional scaling of the individual voxel-wise ^{18}FDG uptake to white matter (given the obvious involvement of grey matter on visual analysis; SPM tissue probability map, white matter probability $> 50\%$). Age was included as a covariate and results were thresholded at a false discovery rate (FDR)-corrected *P*-value of 0.01. Second, to exclude that the results were biased by the use of a necessarily pragmatic control group, we repeated the analysis using a group ($n = 35$) of age-matched healthy volunteers from the Alzheimer's disease neuroimaging initiative (ADNI) database, who were scanned with a state-of-the-art conventional PET system from the same vendor as in the present study (Gemini TF PET/CT; Philips Healthcare) at their ADNI baseline visit. PET scans of the COVID-19 patients were downscaled to the matrix of the ADNI controls ($2 \times 2 \times 2$ mm^3). All scans were smoothed with a Gaussian filter of 8 mm full-width at half-maximum and analysed with a Scaled Subprofile Modelling/PCA routine in analogy to the methods described above.

CSF analysis

In the case of lasting confusion or cranial nerve palsy, CSF was analysed with routine parameters (i.e. cell count, glucose, lactate, total protein, protein level/quotient, albumin level/quotient, oligoclonal bands in CSF/serum and immunoglobulin A/M/G levels/quotients). In addition, RT-PCR for SARS-CoV2 was performed.

Neuropathological examination

One patient died due to an extracerebral cause. Macroscopic and microscopic examinations of the brain were performed according to standard procedures by a board-certified neuropathologist (M.P.) (Supplementary material).

Statistical analysis

Statistical analyses were performed using IBM SSPS Statistics version 25 (Ehningen, Germany) and R (https://www.R-project.org/). Shapiro-Wilk and Kolmogorov-Smirnov tests were used to confirm the normal distribution of datasets. For group comparisons Student's *t*-tests were applied.

Data availability

Data and code are available from the authors upon reasonable request.

Results

Patients characteristics and symptomatology of the Neuro-COVID-19 cohort

Forty-one COVID-19 patients requiring inpatient treatment were prospectively screened. Six patients were excluded because of premorbid neurodegenerative disorders and one patient because of premorbid multiple sclerosis. Four patients declined to participate in the register. Of the remaining patients, only one did not display any neurological symptoms. Thus, we report the data from 29 patients meeting the inclusion criteria for the Neuro-COVID-19 register. Reasons for inpatient treatment, demographic characteristics and basic clinical data are listed in Table 1. The details of patient enrolment are illustrated in Fig. 1.

New neurological symptoms as defined by the inclusion criteria were distributed as follows: gustatory impairment in all patients (29/29), impairment of smell in 25/29 patients (15 patients with hyposmia and 10 patients with anosmia) and impaired performance on the MoCA in 18/26 patients (the three remaining patients refused the MoCA). Other symptoms occurred less frequently, e.g. affection of cranial nerve VI, VII and VIII in one patient each or cortical symptoms (1/29; aphasia and right-sided neglect). The complete results of the neurological examination are presented in Table 2. Additional anamnestic data are reported in Supplementary Table 2. Of the patients in the register, 26 of

29 had two or more new neurological symptoms during their COVID-19 infection, indicating eligibility for an extended examination including multimodal imaging and detailed neuropsychological testing. The allocation to extended diagnostics is displayed in Fig. 1 and Supplementary material.

Cognitive functions

Of patients performing below the cut-off in the MoCA test, 14 (54%) were mild to moderately impaired (MoCA 18–25) and four (15%) were severely impaired (MoCA 10–17). The MoCA domain scores revealed particular impairment in the domains of executive abilities, visuoconstruction, memory and attention (Table 2, for single item scores see Supplementary Table 3). Language and orientation were not impaired.

A total of 15 of 29 patients underwent extended neuropsychological testing; only two patients performed entirely normally. The Word list learning on the Hopkins Verbal Learning Test–Revised (representing the cognitive domain memory) was affected most frequently (7/14) as were executive functions [digit span reverse (6/15); categorical fluency (6/13)]. Tests for attention were less frequently impaired (Table 3, diverging total numbers resulted from the fact that individual patients did not complete all tests in the battery). These findings to a large part confirmed the results from the MoCA.

Table 1 Demographic characteristics and basic clinical data

	n (%) or mean (SD)
Total number of patients in the register	29 (100%)
Sex male/female	18 (62%)/11 (38%)
Age, years	65.2 (14.4)
Years of education, years	13.2 (3.0)
Δ Symptom onset: clinical examination, days	18.4 (2.3)
Δ Symptom onset: MoCA (*n* = 26), days	18.4 (2.3)
Δ Symptom onset: neuropsychological test battery (*n* = 15), days	29.6 (13.6)
Δ Symptom onset: ^{18}FDG PET (*n* = 15), days	31.2 (13.9)
Δ Symptom onset: cMRI (*n* = 13), days	30.5 (13.4)
Reason for inpatient treatment	
Reduced general condition	10 (35%)
Organ failure	6 (21%)
Bacterial pulmonary superinfection	5 (17%)
Malignancies	3 (10%)
Post-surgery in-hospital infection	3 (10%)
Endocarditis	1 (3%)
Ischaemic stroke	1 (3%)
Required immunosuppression	7 (24%)
Past ICU treatment	
Only observation	2 (7%)
Non-invasive ventilation	2 (7%)
Endotracheal ventilation	3 (10%)
Short-term follow-up	
Discharge home	22 (76%)
Discharge to rehabilitation clinic	5 (17%)
Still hospitalized due to persistent infectivity	1 (3%)
Died	1 (3%)

Cerebral MRI

In total, 13/29 patients underwent cerebral MRI (Fig. 1); contrast agent administration was omitted in two patients because of chronic kidney disease. In four patients (30%), microembolic subacute infarcts were observed (n = 1 bilateral cerebellar; in n = 1 each, pinhead-sized lesions were located in the right corona radiata, the left superior cerebellar peduncle and the right frontal cortex). No other structural changes, and in particular no sign of atrophy, acute encephalitis or leptomeningeal enhancement, were found. Region of interest-based analysis of DSC-perfusion did not reveal significant differences when compared with a control group (only a trend effect was observed for left temporal cerebral blood flow, P = 0.089). The voxel-based analysis of DSC-perfusion did not show differences (at 5% FDR, corresponding to $P < 0.001$ uncorrected).

^{18}FDG PET imaging

Fifteen of 29 patients underwent cerebral ^{18}FDG PET (Fig. 1). Individual ratings of both observers were normal (0) in five and six, mildly abnormal (1) in six and five and severely abnormal (2) in four cases each, respectively. Of note, these ratings accounted for known small bilateral cerebellar infarctions and an addition old occipital infarction in one patient each. The other three pinhead-sized infarctions were not recognizable on PET. The raters agreed in 10 cases and differed by no more than one step in five cases (weighted kappa = 0.61). In consensus, 10 of 15 patients (67%) were judged to show an overall pathological result.

Concerning the dominant pathological findings, rater 1 noted cortical hypometabolism in 10/10 pathological scans (with frontal, parietal and fronto-parietal pronunciation in two each), accompanied by relative striatal hypermetabolism in two cases. Rater 2 noted cortical hypometabolism in 6/9 pathological scans (emphasis: frontal, frontotemporal and parietal in one case and fronto-parietal in two cases) and hypermetabolism of the striatum in the remaining three cases (plus hypermetabolism of vermis in one case). No pattern clearly suggestive of neurodegenerative disease as an alternative explanation of cognitive impairment was observed. The individual ^{18}FDG PET scans are shown in Fig. 2.

In the PCA group analysis, the first six principal components (PCs) accounted for 55% of the total variance. PC 1 and 5 showed significant group differences ($P < 0.05$); PC 1 showed a significant group difference after Bonferroni adjustment ($P < 0.001$) and was selected as it explained 22.2% of the total variance (predefined threshold of 5%; PC 5: 4.1%). The resulting COVID-19-related pattern showed highly significant separation between the COVID-19 patients and control patients ($P < 0.001$). The averaged

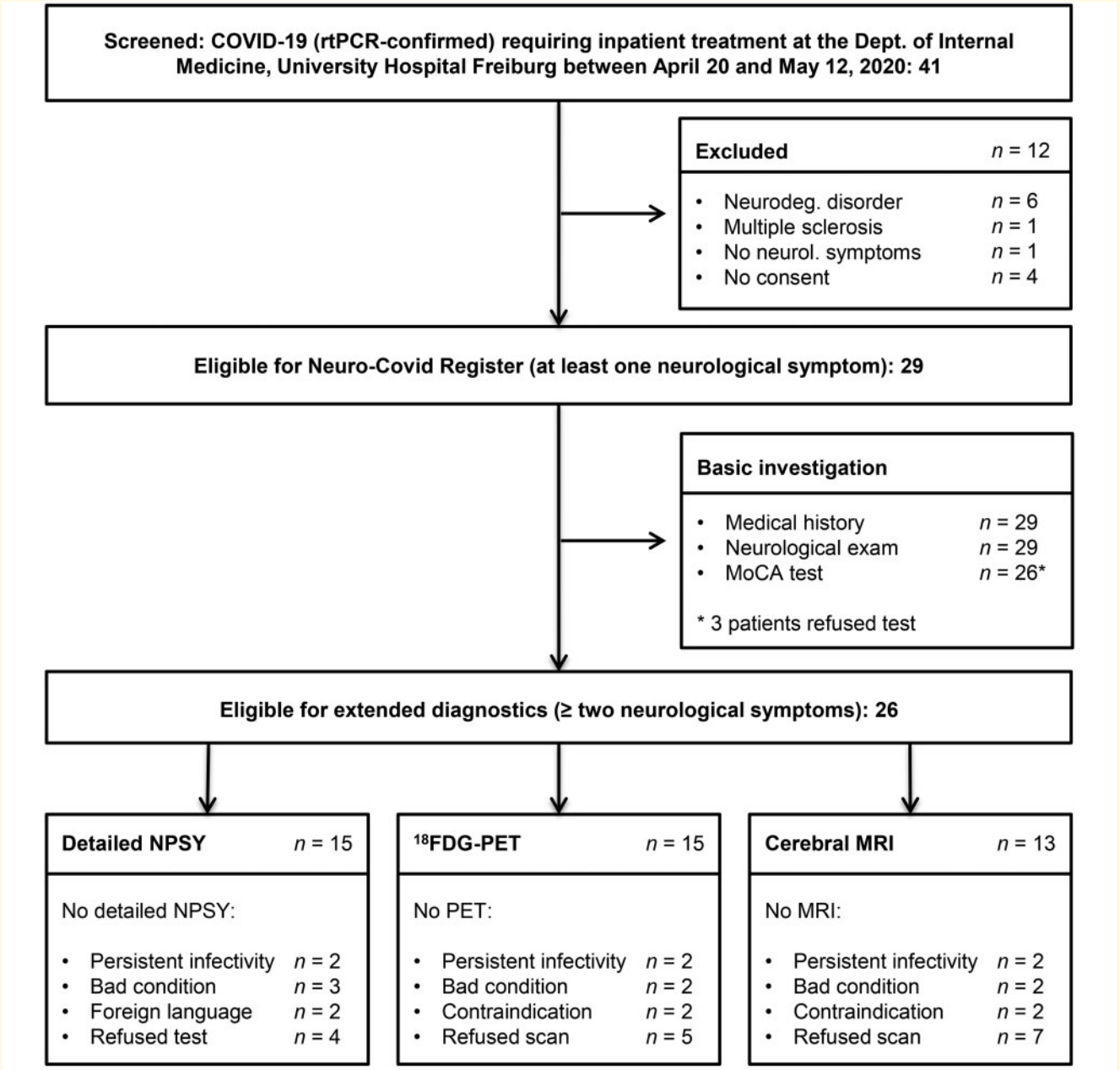

Figure 1 Flow chart indicating the enrolment of COVID-19 patients and the investigations that were performed. NPSY = detailed neuropsychological battery.

^{18}FDG PET images of the two groups and the COVID-19-related spatial covariance pattern of cerebral glucose metabolism are shown in Fig. 3. Voxels with negative weights involve extensive neocortical areas with regional pronunciation in parietal and frontal association cortices and, to a lesser extent, caudate nuclei. Conversely, voxels with positive weights cover extensive areas of brainstem, cerebellum, white matter and mesial temporal lobe structures (i.e. allocortex and the transitional zone proisocortex).

Exploratory regional analyses showed no significant difference (+3.5%) between the mean SUV (surrogate of regional glucose metabolism) of areas with positive weights in COVID-19 patients and control patients [mean SUV of voxel with 10% highest weights: 378.3 (49.1) versus 365.5 (49.2) g/ml × mg/dl, $P = 0.39$, two-tailed t-test]. In contrast, voxels with negative weights showed a tendency towards significantly lower (–9.4%) group average SUV values in COVID-19 patients compared with control patients [mean SUV of voxels with 10% highest weights: 502.5 (103.4) versus 554.5 (90.9) g/ml × mg/dl, $P = 0.097$]. In line with the visual reads and average group images, this supported the notions that voxels with negative weights represent areas of

Table 2 Results of the neurological examination and MoCA

	Total *n*	*n* with deficit (%) or mean (SD)
Olfaction		
Anosmia	29	10 (34%)
Hyposmia	29	15 (52%)
Average correct odour perception (12 items)	29	7.7 (2.8)
Gustation		
Hypogeusia	29	29 (100%)
Average correct perception of taste (4 items)	29	1.8 (1.0)
Other cranial nerves		
Abducens nerve palsy	29	1 (3%)
Facial nerve palsy	29	1 (3%)
Peripheral vestibular dysfunction	29	1 (3%)
Sensorimotor function		
Slight hemiparesis	29	1 (3%)
Babinski sign positive	29	1 (3%)
Dysmetric attempted pointing	29	2 (7%)
Cortical symptoms		
Right-sided multimodal neglect and aphasia	29	1 (3%)
MoCA global score[a] (max. 30)	26	21.77 (5.35)
MoCA global score[a] < 26	18 (69%)	19.11 (4.14)
MoCA global score[a] 18–25	14 (54%)	20.93 (2.05)
MoCA global score[a] 10–17	4 (15%)	12.75 (2.49)
MoCA global score[a] ≧ 26	8 (31%)	27.75 (1.16)
MoCA domain scores		
Orientation (max. 6)	26	5.61 (0.68)
Attention (max. 6)	26	4.58 (1.34)
Language (max. 5)	26	4.54 (0.80)
Executive (max. 4)	26	2.23 (1.30)
Visuoconstructive (max. 4)	26	2.50 (1.34)
Memory (max. 5)	26	1.92 (1.70)

[a]Corrected for years of education.

Table 3 Results of the comprehensive neuropsychological test battery

	n	*n* below –1.5 SD	*Z*-score mean (SD)
Hopkins verbal learning revised (HVLT-R)			
HVLT-R total	14	7	–1.30 (1.21)
HVLT-R delayed recall	14	6	–0.90 (0.98)
HVLT-R delayed recognition	14	2	–0.24 (0.99)
Trail Making Test			
Trail making A	15	2	0.21 (1.28)
Trail making B	15	3	–0.36 (1.23)
Stroop test			
Stroop test Word reading	14	4	–0.36 (1.22)
Stroop test: Color naming	14	2	–0.16 (1.08)
Stroop test: Interference	14	2	–0.07 (1.02)
Digit span			
Digit span forward	15	3	–1.05 (0.86)
Digit span reverse	15	6	–0.69 (1.01)
Symbol digit modalities test	14	2	–0.57 (1.04)
Fluency			
Categorical (animals)	13	6	–1.05 (1.40)
Phonemic (s-words)	13	3	–0.42 (1.24)

decreased cerebral glucose metabolism, whereas those with positive weights indicate areas with preserved rather than increased metabolism.

As expected, the pattern expression score was significantly higher in COVID-19 patients [33.9 (49.9)] compared with the control patients [–11.3 (28.8); $P < 0.001$ with adjustment for the subjects' age]. Visual reads in COVID-19 patients correlated significantly with the pattern expression score (rank correlation coefficient $r = 0.80$, $P < 0.001$ and 0.71, $P = 0.003$ for rater 1 and 2, respectively). Finally, there was a highly significant linear relationship between cognitive assessment (MoCA global score adjusted for years of education) and PET ($R^2 = 0.62$, $P < 0.001$; i.e. a higher pattern expression score was associated with worse cognitive performance; Fig. 4).

For further validation, we conducted a conventional group analysis using SPM and white matter as a reference region (given the obvious involvement of grey matter on visual analysis). Voxels that showed a significant decrease of regional glucose metabolism in COVID-19 patients compared with the controls (FDR-corrected $P < 0.01$) are displayed in Fig. 5A. The pattern of widespread, frontoparietal dominant

neocortical hypometabolism was similar to the result from the PCA. Of note, exploratory regional analysis using the aforementioned significant SPM clusters revealed a significant decline (-12.4%; $P = 0.01$) in regional SUV as a surrogate of regional glucose metabolism in the group of COVID-19 patients (488.5 ± 88.1 g/ml × mg/dl) compared to the group of control patients (557.9 ± 86.9 g/ml × mg/dl). No voxels with significant increases in ^{18}FDG uptake survived the FDR correction.

To exclude that results were biased by using a necessarily pragmatic control group, we repeated the PCA analysis using a group ($n = 35$) of age-matched healthy volunteers from the ADNI database. The first four PCs accounted for 51.8% of total variance. PC 1 and 3 showed significant group differences ($P < 0.05$), of which only PC 1 showed a significant group difference after Bonferroni adjustment ($P < 0.001$) and was selected as it explained most of total variance (31.9%). The resulting COVID-19-related pattern showed a highly significant separation between COVID-19 patients and control patients ($P = 2.3 \times 10^{-14}$). The COVID-19-related spatial covariance pattern based on comparison with ADNI controls is shown Fig. 5B. Voxels with negative weights involve extensive neocortical areas with regional pronunciation in parietal and frontal association cortices and, to a lesser extent, caudate nuclei. Conversely, voxel with positive weights cover extensive

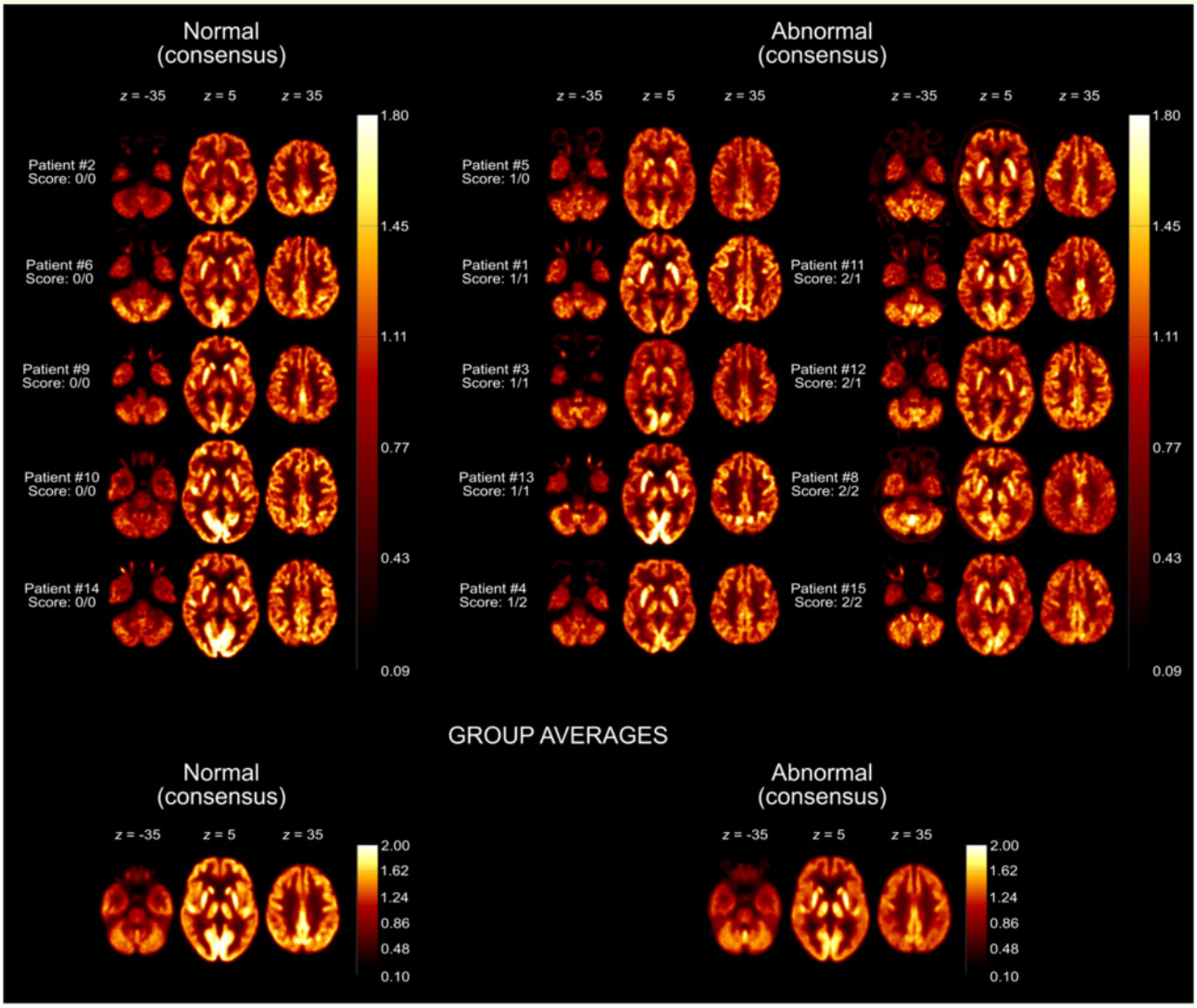

Figure 2 Individual ^{18}FDG PET scans grouped according to the visual ratings. Transaxial ^{18}FDG PET images of COVID-19 patients that were rated as normal (*left column*) or abnormal (*middle and right columns*) in consensus. Image count rates were normalized to total brain parenchyma for comparable display (see heat bars) in analogy to the procedure used in clinical routine [radiological orientation, i.e. left image side corresponds to patient's right body side; numbers denote the axial (z) position in millimetres; scores denote the results of visual ratings separately for each rater]. The last row shows transaxial sections of group-averaged spatially-normalized ^{18}FDG PET scans. Given the apparent involvement of grey matter on individual visual reads, all scans were normalized to white matter (SPM white matter mask, white matter probability > 50%) for the calculation of group averages.

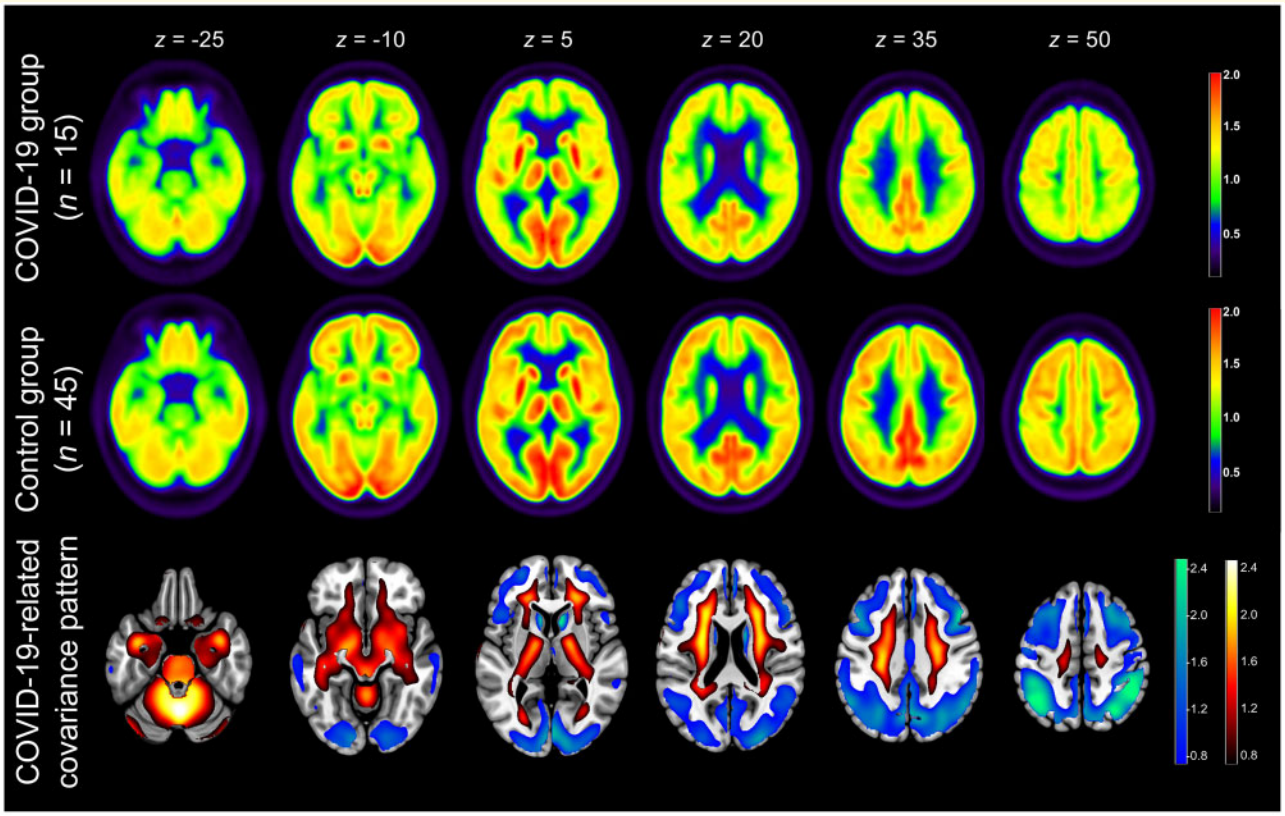

Figure 3 Result of ^{18}FDG PET group analysis. *Top and middle row*: Transaxial sections of group averaged, spatially normalized ^{18}FDG PET scans in COVID-19 patients and controls. Given the apparent involvement of grey matter on individual visual reads, all scans were normalized to white matter (SPM white matter mask, white matter probability > 50%). *Bottom row*: COVID-19-related spatial covariance pattern of cerebral glucose metabolism constructed by PCA of the aforementioned groups. For illustration purposes, the spatial covariance pattern was restricted to voxels of the highest quartile of covariance of voxel weights (positive and negative; note that all brain voxels contribute to the pattern expression score according to their weights) and overlaid onto an MRI template. Voxels with negative region weights are colour-coded in cool colours, and regions with positive region weights in hot colours [neurological orientation, i.e. left image side corresponds to patient's left body side; numbers denote the axial (z) position in millimetres].

areas of brainstem, cerebellum, white matter and mesial temporal lobe structures. Note that the identified covariance pattern was similar to the results from our primary analysis based on the control patients, albeit the difference between scanners introduced some additional deviation of signal (see higher variance explained, lower *P*-value for group separation).

CSF analyses

CSF samples were obtained from 4/29 patients (two with cranial nerve palsy and two with lasting confusion). The cell count was normal except in one patient (abducens nerve palsy) who showed a lymphocytic pleocytosis (8 cells/µl). In one patient (lasting confusion) oligoclonal bands were present with identical electrophoretic patterns in the serum. Otherwise, routine parameters including protein and immunoglobulin G levels were normal. RT-PCR results from the CSF samples were negative for SARS-CoV-2 in all patients.

Neuropathological findings

Post-mortem assessment of the brain of one patient who died due to an extracerebral cause (suspicion of aspiration pneumonia) revealed a pronounced microgliosis including formation of microglia nodules. As only a few parenchymal T cells were present, neuroinflammation could not be diagnosed (Prinz and Priller[28]; see Supplementary material for detailed information). Corresponding results from the ^{18}FDG PET, which was performed 22 days before death, are presented in Fig. 2 (Patient 8). Changes were most prominent in the white matter of the cerebellum, hippocampal formation and—to a lesser extent—in the white matter of the frontal cortical tissue (Fig. 6). Thus, microgliosis was confined to white matter, whereas cortical grey matter was mostly spared.

Discussion

The present prospective register study highlights neocortical dysfunction as a neurological sequela of COVID-19 by

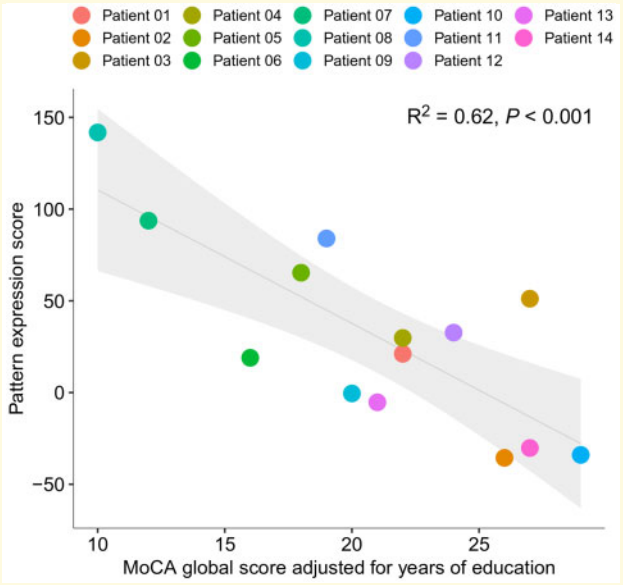

Figure 4 Association between the expression of COVID-19-related covariance pattern (quantified by the so-called pattern expression score; see text) and the MoCA score adjusted for years of education. Each dot represents an individual patient's data; the line (grey shaded area) corresponds to the fit of a linear regression (95% confidence interval; see Figure for R^2 and *P*-value).

identifying cognitive decline in COVID-19 inpatients at the subacute stage using comprehensive neuropsychological testing and functional imaging with ^{18}FDG PET. Although the selection of the present cohort (affected severely enough to require inpatient, but not dominant ICU treatment and short time window of data collection) limits generalizability, these findings may be of considerable rehabilitative and socioeconomic relevance.

Our register included COVID-19 inpatients showing affection of gustation and olfaction, cognitive impairment and/or other neurological signs. Of importance, performance in the MoCA test was impaired in 18 of 26 COVID-19 patients tested. This indicates that besides cranial nerve affection and other neurological symptoms that were reported previously,[1,29] cognitive deficits are present in many COVID-19 patients requiring inpatient treatment. With an average score of 21.8/30, the MoCA indicates mild to moderate cognitive impairment in our cohort. At first glance, this finding could be a non-specific consequence of a reduced general condition in critically ill patients. However, there are two reasons arguing against this hypothesis. First, the orientation and language abilities on the MoCA in COVID-19 patients were in the range of healthy subjects,[21] whereas memory and executive items were most severely affected (Table 2), which makes general deterioration unlikely. The extended neuropsychological test battery corroborates the decline in

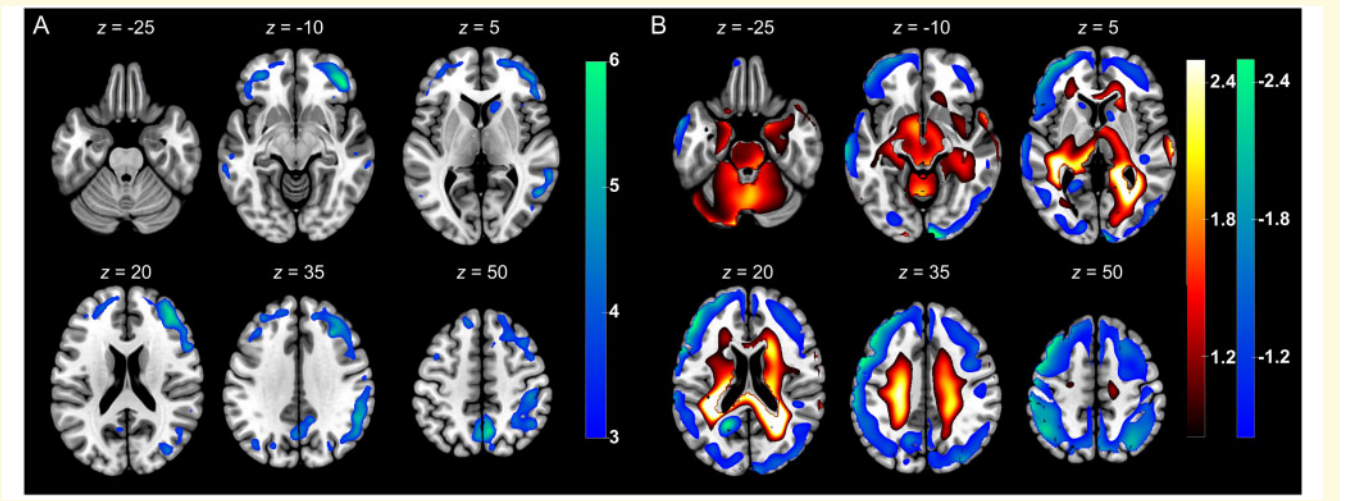

Figure 5 Results of confirmatory ^{18}FDG PET analyses. (**A**) Results of confirmatory SPM analysis. Illustrated are regions that showed significant decreases of normalized ^{18}FDG uptake in COVID-19 patients compared to control patients [SPM (T) values are colour-coded and overlaid onto an MRI template; two-sample *t*-test adjusted for age, FDR $P < 0.01$; neurological orientation, i.e. left image side corresponds to patient's left body side; numbers denote the axial (z) position in millimetres]. (**B**) Results of confirmatory PCA relying on healthy controls from the ADNI database. Shown are voxels of the highest quartile of covariance voxel weights, both for negative and positive voxel weights, of the COVID-19 related covariance pattern overlaid onto an MRI template [voxels with negative region weights are colour-coded in cool colours, those with positive region in hot colours; neurological orientation, i.e. left image side corresponds to patient's left body side; numbers denote the axial (z) position in millimetres].

memory and executive functions but not in general attention or processing speed (Table 3). This specific pattern can hardly be explained by non-specific factors like fatigue. It also differs from cognitive impairment post sepsis,[30] where attention and processing speed are also impaired.[31] This suggests an involvement of frontoparietal cortical areas.[32] Second, the extensive neuropsychological testing and the ^{18}FDG PET were performed on average 1 month after symptom onset (Table 1) at a time when patients had surmounted the acute symptoms of COVID-19 (including pulmonary complications or organ failure) and were close to being discharged from hospital.

Other clinical outcome parameters corroborate the results from previous studies in COVID-19 patients.[3,4,29] However, the frequency of neurological symptoms in our sample of COVID-19 patients was higher than that found in a previous report of an inpatient cohort (i.e. 37%[3]) which can probably be explained by the designs of the studies (i.e. retrospective review of electronic medical records versus prospective examination by experienced neurologists in the present study).

We used ^{18}FDG PET to unravel the neuronal correlates of cognitive decline in COVID-19 patients: visual reads of individual patients' ^{18}FDG PET scans yielded abnormal results of two-thirds of patients with predominant frontoparietal hypometabolism. We also observed an apparently increased ^{18}FDG uptake in striatum and vermis in some cases, which, however, probably reflects a relative image pattern shift towards preserved cerebral structures (i.e. relative hypermetabolism in the case of cortical hypometabolism). To investigate a COVID-19-related spatial covariance pattern, we employed PCA as an advanced statistical image analysis that takes advantage of the entire image data at once instead of parcelling the brain into numerous voxels or regions as in conventional analyses. We detected a highly significant COVID-19-related spatial covariance pattern that is characterized by positive weights in brainstem, cerebellum, white matter and mesiotemporal structures and negative weights in wide-spread neocortical areas. The expression of this pattern was highly correlated (R^2 = 0.62) with cognitive function as assessed by the MoCA. Of note, we found no clear evidence for regional hypermetabolism possibly indicating cerebral inflammation. Future studies with specific imaging agents (e.g. TSPO ligands) may provide deeper insight into a possible inflammatory affection of the CNS.

In contrast with ^{18}FDG PET imaging, structural imaging using cerebral MRI revealed no relevant abnormalities on structural or perfusion-weighted images (including DSC-perfusion analysis). However, 4/13 scans showed microembolic subacute infarcts, which is in line with a previous imaging

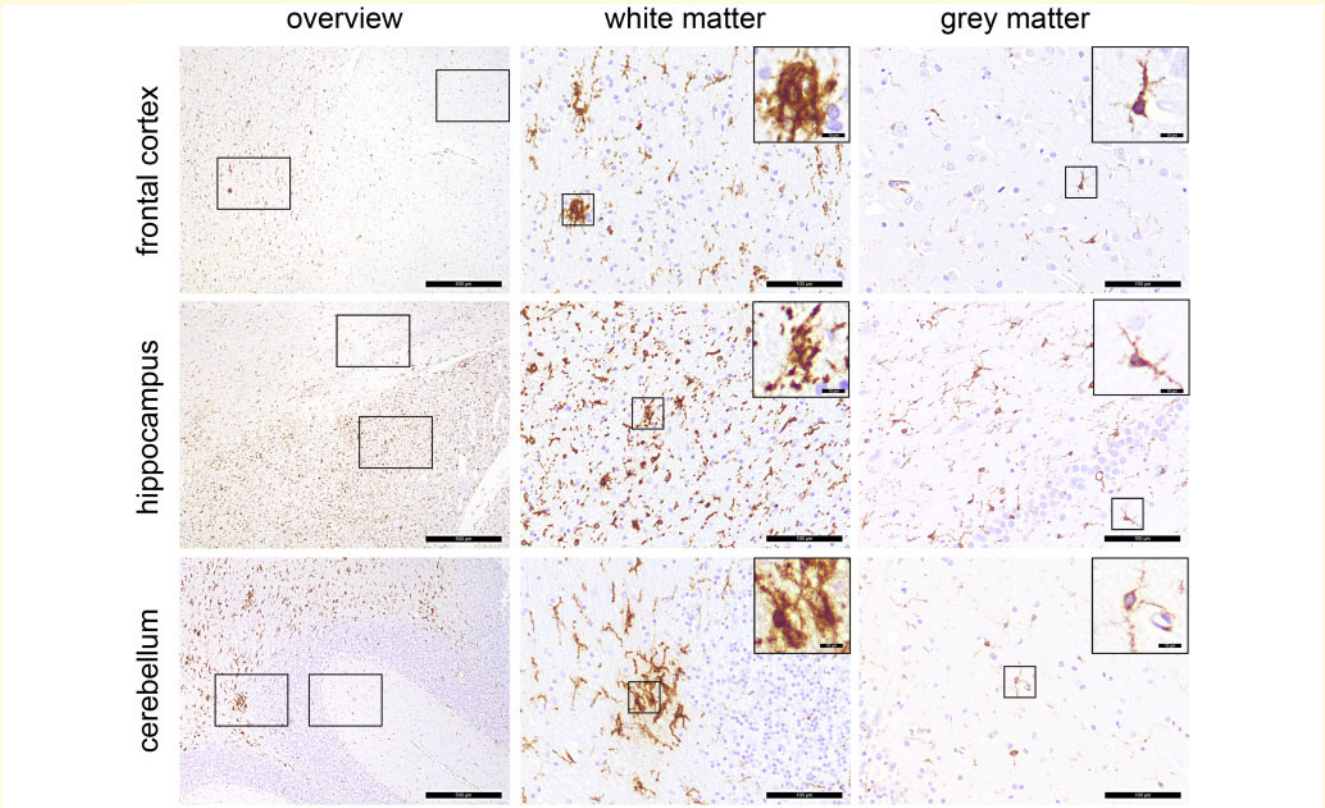

Figure 6 Distribution pattern of microglia activation. Immunohistochemical reactions for human leukocyte antigen DR isotype (brown), counterstaining with haematoxylin (blue) in different regions of the CNS. Microgliosis and formation of microglia nodules are confined to the white matter, whereas grey matter regions are largely unaffected. Scale bars = 500 μm, 100 μm and 10 μm in the *insets*, respectively.

series in COVID-19 patients.[3] Importantly, only one patient showed clinical signs of cerebral ischaemia and the distribution of the present small and asymptomatic lesions can neither explain the cognitive impairments nor the pattern of cortical hypometabolism revealed by ^{18}FDG PET. Acute signs of a systemically triggered local inflammatory response, such as perfusion abnormalities or leptomeningeal contrast enhancement,[4] were absent in our study, possibly as they had already resolved at the time point of 30.5 days after symptom onset.

Post-mortem neuropathology in one of our patients found no evidence of irreversible neocortical damage but pronounced microglia activation within white matter that largely spared cortical grey matter. Of note, there were also no signs of hypoxic or haemorrhagic damage as reported by others.[33] Thus, frontoparietal cortical hypometabolism might rather be a sequel of a remote process due to brainstem or white matter pathology than direct cortical damage (e.g. decoupling from or dysfunction of strategic regions like aminergic brainstem nuclei). This also suggests that neurological deterioration may be reversible, which underlines the need for follow-up studies that will also clarify the possible role of ^{18}FDG PET for monitoring and prognosis.

A broad spectrum of neuronal syndromes including encephalopathies, encephalitic syndromes, acute disseminated encephalomyelitis with haemorrhage and necrotic change, transverse myelitis or Guillain-Barré syndrome has been associated with COVID-19.[1] This variety of manifestations points to different underlying pathophysiological mechanisms induced by the SARS-CoV-2 infection. Apart from direct viral damage, post-infectious inflammation, production of anti-neuronal autoantibodies, vasculitis, cytokine-related hyperinflammation and the cerebral complications of hypoxia and coagulopathy have been discussed.[1,34-36] In our cohort, cerebral MRI did not reveal any signs of demyelination or vasculitic lesions and the lack of a clear-cut regional hypermetabolism in ^{18}FDG PET argues against active encephalitis. Together with our pathological sample that indicates innate immune activation, a systemic cytokine release or cytokine-related hyperinflammation[15,35] may be a valid explanation for cortical dysfunction, leading to cerebral hypometabolism and cognitive impairment. Similar to septic encephalopathies after bacterial infections, a systemic immune response triggers an inflammatory reaction within the brain leading for example to disruption of the blood–brain barrier, impaired astrocytic clearance at synapses and disturbed microcirculation.[7] Cortical hypometabolism was reported in a rat model of sepsis[37] and also in patients suffering from infection-associated delirium,[38] but this phenomenon resolved with convalescence. Although COVID-19 patients were scanned (on average) one month after first symptoms occurred, cortical hypometabolism could be the remnant of inflammatory processes triggered by a systemic immune-response. Although less likely, direct viral damage has to be discussed as an alternative pathophysiological model. The neuroinvasive potential of betacoronaviruses is well documented.[10-12] SARS-CoV, which is in the same clade as SARS-CoV-2, could be detected in the brain tissue of patients who died of severe acute respiratory syndrome (SARS) during the 2003 epidemic.[39] After nasal inoculation of HCoV-OC43, another betacoronavirus, viral particles were shown to enter the CNS via axonal transport along olfactory fibres and other cranial nerves through trans-synaptic neuron to neuron propagation.[10] The fact that SARS-CoV-2 is able to replicate in neuronal cells[40] and infects human brain organoids[36] highlights the neurotropism of this viral agent. The high rate of disturbed smell and taste in our registry would be in line with the hypothesis of a neuroinvasion along olfactory or gustatory fibres. On the other hand, disturbed smell and taste may have been caused by a dysfunction of olfactory epithelial support cells independent of neural affection.[41]

Interestingly, elevated serum levels of the neurofilament light chain protein, a marker of axonal injury, have been detected in mild-to-moderate[5] and moderate-to-severe cases of COVID-19.[6] Furthermore, elevated levels of GFAP as a marker of astrocytic activation have been reported in moderate-to-severe cases of COVID-19.[6] Thus, glial activation and affection of axonal integrity seem to occur in response to SARS-CoV-2 infection. However, levels of neurofilament light chain protein remained normal in a COVID-19 patient that suffered from steroid-responsive encephalitis[42] and correlations between neurofilament light chain protein or GFAP levels and neurological manifestations are lacking so far.

With respect to limitations, we are aware that MoCA testing gives limited information about overall cognitive performance but not about detailed neuropsychological syndromes. This problem was addressed by the additional use of a comprehensive neuropsychological test battery. Here, our data might convey a selection bias towards better performance, as only younger and healthier subjects were able to or agreed to complete the neuropsychological test battery. In general, however, MoCA serves as a valid and easily applicable assessment, which has previously been shown to be useful in detecting global cognitive impairment in different groups of patients.[32]

In addition, we did not comprehensively assess CSF markers for neuronal injury and neurodegeneration (CSF was available in only four patients) or serum markers for neuronal injury (e.g. neurofilament light chain protein). Such parameters should be considered systematically in future studies investigating neuronal affection in COVID-19. Lastly, we are aware that our cohort is a selective population of COVID-19 inpatients, which does not represent the entire COVID-19 population (in particular, not the less-severely affected patients who did not require inpatient treatment). To assess the burden of cognitive symptoms in all COVID-19 patients, large population-based studies are necessary. However, the present study highlights the fact that physicians treating COVID-19 inpatients should be aware of this phenomenon and include bedside tests evaluating cognitive function (e.g. MoCA) into their routine workup. Patients suffering from cognitive deficits should be presented to neurologists and possibly allocated to cognitive rehabilitation programs.

Acknowledgements

The use in this work of ScAnVP software, copyright © 2020 The Feinstein Institute for Medical Research, is hereby acknowledged. N.S. was funded by the Berta-Ottenstein-Programme for Clinician Scientists, Faculty of Medicine, University of Freiburg. A small proportion (normal controls for validation of primary PET analysis) of data used in the preparation of this article were obtained from the ADNI database (adni.loni.usc.edu). As such, the investigators within the ADNI contributed to the design and implementation of ADNI and/or provided data but did not participate in the analysis or writing of this report. A complete listing of ADNI investigators can be found at: http://adni.loni.usc.edu/wp-content/uploads/how_to_apply/ADNI_Acknowledgement_List.pdf. Data collection and sharing for this project was funded by the ADNI (National Institutes of Health Grant U01 AG024904) and the Department of Defense ADNI (Department of Defense award number W81XWH-12-2-0012). ADNI is funded by the National Institute on Aging, the National Institute of Biomedical Imaging and Bioengineering and through generous contributions from the following: AbbVie, Alzheimer's Association; Alzheimer's Drug Discovery Foundation; Araclon Biotech; BioClinica, Inc.; Biogen; Bristol-Myers Squibb Company; CereSpir, Inc.; Cogstate; Eisai Inc.; Elan Pharmaceuticals, Inc.; Eli Lilly and Company; EuroImmun; F. Hoffmann-La Roche Ltd and its affiliated company Genentech, Inc.; Fujirebio; GE Healthcare; IXICO Ltd.; Janssen Alzheimer Immunotherapy Research & Development, LLC.; Johnson & Johnson Pharmaceutical Research & Development LLC.; Lumosity; Lundbeck; Merck & Co., Inc.; Meso Scale Diagnostics, LLC.; NeuroRx Research; Neurotrack Technologies; Novartis Pharmaceuticals Corporation; Pfizer Inc.; Piramal Imaging; Servier; Takeda Pharmaceutical Company; and Transition Therapeutics. The Canadian Institutes of Health Research is providing funds to support ADNI clinical sites in Canada. Private sector contributions are facilitated by the Foundation for the National Institutes of Health (www.fnih.org). The grantee organization is the Northern California Institute for Research and Education, and the study is coordinated by the Alzheimer's Therapeutic Research Institute at the University of Southern California. ADNI data are disseminated by the Laboratory for Neuro Imaging at the University of Southern California.

Funding

No funding was received towards this work.

Competing interests

P.T.M received honoraria for lectures and consulting by GE and Philips. H.U. is shareholder of the Veobrain Gmbh (a spin-off of the University Medical Centre Freiburg) and received honoraria for lectures from Bracco, Bayer, Union Chimique Belge (UCB) pharma and Stryker. All other authors report no competing interests.

Supplementary material

Supplementary material is available at *Brain* online.

References

1. Paterson RW, Brown RL, Benjamin L, et al. The emerging spectrum of COVID-19 neurology: Clinical, radiological and laboratory findings. *Brain*. 2020;143:3104-3120.
2. Zubair AS, McAlpine LS, Gardin T, et al. Neuropathogenesis and neurologic manifestations of the coronaviruses in the age of coronavirus disease 2019: A review. *JAMA Neurol*. 2020;77:1018.
3. Mao L, Wang M, Chen S, et al. Neurological Manifestations of Hospitalized Patients with COVID-19 in Wuhan, China: A Retrospective Case Series Study. *medRxiv* [Preprint]. doi:10.1101/2020.02.22.20026500.
4. Helms J, Kremer S, Merdji H, et al. Neurologic features in severe SARS-CoV-2 infection. *N Engl J Med*. 2020;382:2268-2270.
5. Ameres M, Brandstetter S, Toncheva AA, et al. Association of neuronal injury blood marker neurofilament light chain with mild-to-moderate COVID-19. *J Neurol*. 2020;267:3476-3478.
6. Kanberg N, Ashton NJ, Andersson L-M, et al. Neurochemical evidence of astrocytic and neuronal injury commonly found in COVID-19. *Neurology*. 2020;95:e1754-e1212.
7. Chung H-Y, Wickel J, Brunkhorst FM, et al. Sepsis-associated encephalopathy: From delirium to dementia? *J Clin Med*. 2020;9:703.
8. Salluh JIF, Wang H, Schneider EB, et al. Outcome of delirium in critically ill patients: Systematic review and meta-analysis. *BMJ*. 2015;350:h2538.
9. Troyer EA, Kohn JN, Hong S. Are we facing a crashing wave of neuropsychiatric sequelae of COVID-19? Neuropsychiatric symptoms and potential immunologic mechanisms. *Brain Behav Immun*. 2020;87:34-39.
10. Desforges M, Le Coupanec A, Dubeau P, et al. Human coronaviruses and other respiratory viruses: Underestimated opportunistic pathogens of the central nervous system? *Viruses*. 2019;12:14.
11. Dubé M, Le Coupanec A, Wong AHM, et al. Axonal transport enables neuron-to-neuron propagation of human coronavirus OC43. *J Virol*. 2018;92:e00404-18.
12. Li Y, Bai W, Hashikawa T. The neuroinvasive potential of SARS-CoV2 may be at least partially responsible for the respiratory failure of COVID-19 patients. *J Med Virol*. 2020;92:552-555. jmv.
13. Hornuss D, Lange B, Schröter N, et al. Anosmia in COVID-19 patients. *Clin Microbiol Infect*. 2020;26:1426-1427.
14. Lechien JR, Chiesa-Estomba CM, De Siati DR, et al. Olfactory and gustatory dysfunctions as a clinical presentation of mild-to-moderate forms of the coronavirus disease (COVID-19): A multicenter European study [Internet. *Eur Arch Otorhinolaryngol*. 2020;277:2251-2261.
15. Huang K-J, Su I-J, Theron M, et al. An interferon-?-related cytokine storm in SARS patients. *J Med Virol*. 2005;75:185-194.
16. Kennedy C, Des Rosiers MH, Jehle JW, et al. Mapping of functional neural pathways by autoradiographic survey of local metabolic rate with (14C)deoxyglucose. *Science*. 1975;187:850-853.
17. Jack CR, Bennett DA, Blennow K, et al. NIA-AA Research Framework: Toward a biological definition of Alzheimer's disease. *Alzheimers Dement*. 2018;14:535-562.
18. Graus F, Titulaer MJ, Balu R, et al. A clinical approach to diagnosis of autoimmune encephalitis. *Lancet Neurol*. 2016;15:391-404.

19. Kobal G, Hummel T, Sekinger B, et al. 'Sniffin' sticks': Screening of olfactory performance. *Rhinology*. 1996;34:222-226.
20. Hüttenbrink KB, Damm L. AWMF-Leitlinie "Riech- und Schmeckstörungen". In: Leitliniensammlung. Stuttgart: Thieme; 2020.
21. Nasreddine ZS, Phillips NA, Bédirian V, et al. The Montreal cognitive assessment, MoCA: A brief screening tool for mild cognitive impairment: MOCA: A BRIEF screening tool for MCI. *J Am Geriatr Soc*. 2005;53:695-699.
22. Lazar RM, Pavol MA, Bormann T, et al. Neurocognition and cerebral lesion burden in high-risk patients before undergoing transcatheter aortic valve replacement. *JACC Cardiovasc Interv*. 2018; 11:384-392.
23. Varrone A, Asenbaum S, Vander Borght T, et al. EANM procedure guidelines for PET brain imaging using [18F]FDG, version 2. *Eur J Nucl Med Mol Imaging*. 2009;36:2103-2110.
24. Speck I, Arndt S, Thurow J, et al. 18F-FDG PET imaging of the inferior colliculus in asymmetric hearing loss. *J Nucl Med*. 2020;61: 418-422.
25. Eidelberg D. Metabolic brain networks in neurodegenerative disorders: A functional imaging approach. *Trends Neurosci*. 2009;32: 548-557.
26. Blazhenets G, Ma Y, Sörensen A, et al. Principal components analysis of brain metabolism predicts development of Alzheimer dementia. *J Nucl Med*. 2019;60:837-843.
27. Spetsieris PG, Eidelberg D. Scaled subprofile modeling of resting state imaging data in Parkinson's disease: Methodological issues. *NeuroImage*. 2011;54:2899-2914.
28. Prinz M, Priller J. The role of peripheral immune cells in the CNS in steady state and disease. *Nat Neurosci*. 2017;20:136-144.
29. Romoli M, Jelcic I, Bernard-Valnet R, et al.; For the Infectious Disease Panel of the European Academy of Neurology. A systematic review of neurological manifestations of SARS-CoV-2 infection: The devil is hidden in the details. *Eur J Neurol*. 2020;27: 1712-1726.
30. Brown SM, Collingridge DS, Wilson EL, et al. Preliminary validation of the montreal cognitive assessment tool among sepsis survivors: A prospective pilot study. *Ann Am Thorac Soc*. 2018;15: 1108-1110.
31. Calsavara AJC, Nobre V, Barichello T, et al. Post-sepsis cognitive impairment and associated risk factors: A systematic review. *Aust Crit Care*. 2018;31:242-253.
32. Julayanont P, Nasreddine ZS. Montreal Cognitive Assessment (MoCA): Concept and clinical review. In: AJ Larner, ed. *Cognitive screening instruments*. Cham: Springer International Publishing; 2017:139-195.
33. Solomon IH, Normandin E, Bhattacharyya S, et al. Neuropathological features of Covid-19. *N Engl J Med*. 2020;383: 989-992.
34. Becker RC. COVID-19-associated vasculitis and vasculopathy. *J Thromb Thrombolysis*. 2020;50:499-511.
35. Mehta P, McAuley DF, Brown M, et al. COVID-19: Consider cytokine storm syndromes and immunosuppression. *Lancet*. 2020; 395:1033-1034.
36. Song E, Zhang C, Israelow B, et al. Neuroinvasion of SARS-CoV-2 in human and mouse brain. bioRxiv. [Preprint] doi:10.1101/2020.06.25.169946.
37. Semmler A, Hermann S, Mormann F, et al. Sepsis causes neuroinflammation and concomitant decrease of cerebral metabolism. *J Neuroinflammation*. 2008;5:38.
38. Haggstrom LR, Nelson JA, Wegner EA, Caplan GA. 2-^{18}F-fluoro-2-deoxyglucose positron emission tomography in delirium. *J Cereb Blood Flow Metab*. 2017;37:3556-3567.
39. Ding Y, He L, Zhang Q, et al. Organ distribution of severe acute respiratory syndrome(SARS) associated coronavirus(SARS-CoV) in SARS patients: Implications for pathogenesis and virus transmission pathways. *J Pathol*. 2004;203:622-630.
40. Chu H, Chan JF-W, Yuen TT-T, et al. Comparative tropism, replication kinetics, and cell damage profiling of SARS-CoV-2 and SARS-CoV with implications for clinical manifestations, transmissibility, and laboratory studies of COVID-19: An observational study. *Lancet Microbe*. 2020;1:e14-e23.
41. Brann DH, Tsukahara T, Weinreb C, et al. Non-neuronal expression of SARS-CoV-2 entry genes in the olfactory system suggests mechanisms underlying COVID-19-associated anosmia. *Sci Adv*. 2020;6:eabc5801.
42. Pilotto A, Odolini S, Masciocchi S, et al. Steroid-Responsive Encephalitis in Coronavirus Disease 2019. *Annals of Neurology*. 2020;88(2):423-427.